



HFF  
13,3

266

Received May 2001  
Revised October 2002  
Accepted October 2002

# The effects of density extremum and rotation on the onset of thermal instability

J.P. Pascal

*Department of Mathematics, Physics and Computer Science,  
Ryerson Polytechnic University, Toronto, Ontario, Canada*

S.J.D. D'Alessio

*Department of Applied Mathematics, University of Waterloo, Waterloo,  
Ontario, Canada*

**Keywords** *Instability, Temperature, Heat transfer*

**Abstract** *This paper addresses the onset of Bénard convection on a rotating horizontally confined layer of water near the temperature of maximum density that is heated from below. A quadratic relation between temperature and density is assumed near the density extremum. A linear stability analysis is employed to determine the critical conditions for the onset of thermal instability. The resulting eigenvalue problem is numerically solved by expanding the amplitudes of the temperature and velocity perturbations in a truncated eigenfunction and power series. The validity of the principle of exchange of stabilities is proved analytically for a certain case and numerically investigated in general. Plots of the marginal stability curves as well as the variation of the critical Rayleigh number with other dimensionless parameters which naturally arise in the problem are also presented and discussed.*

## 1. Introduction

Bénard convection is a well-known problem in hydrodynamic stability and marks a major success in linear stability theory. It involves a horizontally confined layer of fluid that is heated from below and under the influence of gravity. This configuration will eventually succumb to convective motion once the temperature gradient in the fluid layer exceeds a certain threshold. This problem represents the competing of two forces, the destabilizing effect of buoyancy versus the stabilizing effect of viscosity. The ratio of these opposing forces forms the parameter  $Ra$  which is referred to as the Rayleigh number.

Bénard (1900) simulated the above instability through extensive experiments. Later, Rayleigh (1916) derived the mathematical theory which predicted the onset of instability. The original problem was concerned with a fluid having a linear relationship between density and temperature. While this is a reasonable approximation for many fluids, it is not adequate in dealing with fluids which are known to have a density extremum. The obvious



---

example is, of course, water whose density attains a maximum at 4°C. Near this temperature of maximum density the relationship between density and temperature is well approximated by a quadratic equation.

The aim of the present investigation is to address the consequences of this quadratic density-temperature relationship as well as those of rotation to the stability characteristics for the case where the fluid layer is horizontally confined by stress-free surfaces and the case where the layer is confined by rigid surfaces. The effect of the nonlinear dependence of the density on the temperature in a nonrotating layer has been investigated in several other studies including Hwang *et al.* (1984) and Mollendorf and Jahn (1983). In these previous investigations, the marginally stable state is numerically determined by setting both the real and imaginary parts of the complex growth rate of disturbances to zero. However, this approach is based on the validity of the principle of exchange of stabilities which can only be proved rigorously for the case of a nonrotating fluid layer horizontally confined between free surfaces (Veronis, 1963). In the current investigation, we present an alternate analytical proof to that given in Veronis (1963) and apply numerical methods which allow us to calculate the complex growth rate. We are thus able to numerically verify the validity of the principle of exchange of stabilities in all cases as well as confirm that the neutrally stable state is also marginally stable.

The paper is organised as follows. In the next section, the equations governing the problem are presented along with the corresponding boundary conditions. Following this, in Section 3, a linear stability analysis is performed and the principle of exchange of stabilities is proved. Section 4 is devoted to the numerical methods implemented to solve the resulting eigenvalue problem emerging from the linear stability analysis along with presenting and discussing the numerical results. Finally, a brief conclusion summarizing the results is included in Section 5.

## 2. Formulation of the problem

We consider a two-dimensional, viscous, incompressible layer of fluid of thickness  $d$  that is arranged horizontally with respect to a Cartesian coordinate system. The top and bottom of the layer, located at  $z = d/2$  and  $z = -d/2$ , respectively, are isothermal with the bottom maintained at a higher temperature than the top. The set up is shown in Figure 1. The fluid is initially motionless and we imagine that at time  $t = 0$  the temperature difference between the top and bottom is applied which may then induce thermal convection. We consider separately the cases with and without rotation.

The fluid motion will be governed by the usual conservation of mass, momentum and energy equations. The dimensional equations for the velocity  $\vec{v}' = (u', v', w')$ , pressure  $P'$  and temperature  $T'$  in vector form are

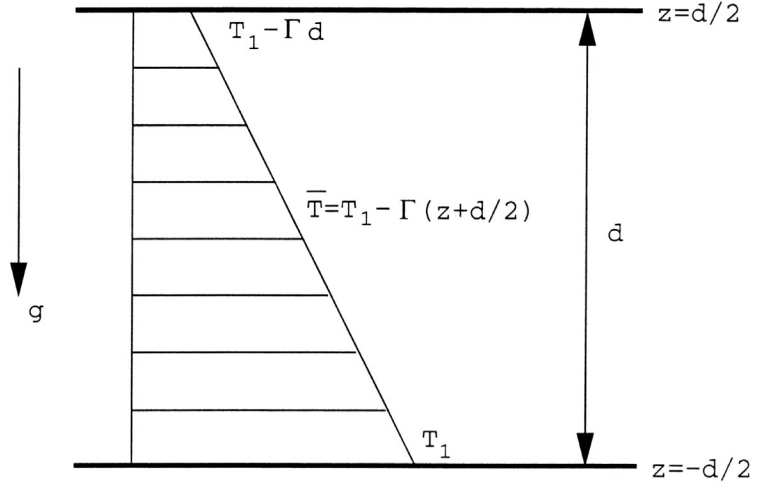


**Figure 1.**  
Sketch of the fluid  
configuration

$$\frac{\partial \vec{v}'}{\partial t} + (\vec{v}' \cdot \nabla) \vec{v}' + f \vec{k} \times \vec{v}' = -\frac{1}{\rho_0} \nabla P' - \frac{\rho'}{\rho_0} g \vec{k} + \nu \nabla^2 \vec{v}', \quad (1)$$

$$\nabla \cdot \vec{v}' = 0, \quad (2)$$

$$\frac{\partial T'}{\partial t} + \vec{v}' \cdot \nabla T' = \kappa \nabla^2 T'. \quad (3)$$

Here,  $g$  denotes the acceleration due to gravity,  $\nu$  the kinematic viscosity,  $\kappa$  the thermal diffusivity,  $\rho_0$  a reference density at temperature  $T_0$  and  $f$  is twice the angular speed of rotation about the  $z$ -axis (denoted by  $\vec{k}$ ). In geophysical applications,  $f$  refers to the Coriolis parameter. In the above equations various assumptions and approximations have been made. These include the Boussinesq approximation, constant fluid properties (with the exception of density) and the neglect of dissipation of mechanical energy into heat. Drazin and Reid (1981) give a lengthy discussion regarding the validity of these assumptions and approximations. For water near the temperature of maximum density,  $T_0 = 4^\circ\text{C}$ , the equation of state, needed to close the above system, is well approximated by the quadratic form (Eklund, 1963)

$$\rho' = \rho_0 \left[ 1 - \frac{\alpha}{2} (T' - T_0)^2 \right]. \quad (4)$$

We next decompose the flow variables into a steady-state part plus an unsteady perturbation as follows:

$$\bar{v}' = \bar{0} + \bar{v}, \quad P' = P(z) + p, \quad T' = \bar{T}(z) + T,$$

where  $P(z)$  represents the hydrostatic pressure and  $\bar{T}(z) = T_1 - \Gamma(z + d/2)$  is the linear steady-state temperature profile across the fluid layer. The constant  $\Gamma$  refers to the magnitude of the vertical temperature gradient and  $T_1$  is the fixed temperature at the bottom of the layer. Substituting these into equations (1) and (3) and linearizing yields

$$\frac{\partial \bar{v}}{\partial t} = -f \bar{k} \times \bar{v} - \frac{1}{\rho_0} \nabla p + \alpha g (\bar{T}(z) - T_0) T \bar{k} + \nu \nabla^2 \bar{v}, \quad (5)$$

$$\frac{\partial T}{\partial t} - \Gamma w = \kappa \nabla^2 T. \quad (6)$$

For the case of a nonrotating fluid layer the corresponding linearised equations are simply obtained by setting  $f = 0$ .

For the case where the fluid layer is horizontally confined by rigid surfaces, the system of equations (5) and (6) is subject to the isothermal and no-slip boundary conditions given by

$$u = v = w = T = 0 \quad \text{at} \quad z = \pm \frac{d}{2}. \quad (7)$$

If the fluid layer is confined by free surfaces then the boundary conditions are

$$w = \frac{\partial u}{\partial z} + \frac{\partial w}{\partial x} = \frac{\partial v}{\partial z} + \frac{\partial w}{\partial y} = T = 0 \quad \text{at} \quad z = \pm \frac{d}{2}, \quad (8)$$

which result from the zero stress and the isothermal conditions.

In the following section, a linear stability analysis is presented and used to determine the conditions under which the steady flow becomes unstable.

### 3. Linear stability analysis

Since previous studies have not included the effects of rotation, the governing equations will be derived. The procedure is standard and similar to that without rotation. We begin by simplifying the linearised equation (5). Taking the Laplacian,  $\nabla^2$ , of the  $z$  component of equation (5) gives

$$\frac{\partial}{\partial t} (\nabla^2 w) = -\frac{1}{\rho_0} \nabla^2 \frac{\partial p}{\partial z} + \nu \nabla^4 w + \alpha g (\bar{T}(z) - T_0) \nabla^2 T - 2\alpha g \Gamma \frac{\partial T}{\partial z}. \quad (9)$$

Next, taking the divergence of equation (9) and making use of equation (2) we obtain

$$0 = -\frac{1}{\rho_0} \nabla^2 p + \alpha g \nabla \cdot [(\bar{T}(z) - T_0) T] \vec{k} - f \zeta, \quad (10)$$

where

$$\zeta = \frac{\partial u}{\partial y} - \frac{\partial v}{\partial x}$$

is the  $z$  component of vorticity. Differentiating the above with respect to  $z$  yields

$$0 = -\frac{1}{\rho_0} \nabla^2 \frac{\partial p}{\partial z} - 2\alpha g \Gamma \frac{\partial T}{\partial z} + \alpha g (\bar{T}(z) - T_0) \frac{\partial^2 T}{\partial z^2} - f \frac{\partial \zeta}{\partial z}. \quad (11)$$

The pressure term can now be eliminated by subtracting equation (11) from equation (9) to arrive at

$$\frac{\partial}{\partial t} (\nabla^2 w) = \nu \nabla^4 w + \alpha g (\bar{T}(z) - T_0) \nabla_H^2 T + f \frac{\partial \zeta}{\partial z}, \quad (12)$$

where

$$\nabla_H^2 = \frac{\partial^2}{\partial x^2} + \frac{\partial^2}{\partial y^2}$$

represents the horizontal Laplacian operator. Lastly, the linearised vorticity equation is

$$\frac{\partial \zeta}{\partial t} = \nu \nabla^2 \zeta - f \frac{\partial w}{\partial z}. \quad (13)$$

Thus, the problem with rotation is governed by equations (6), (12) and (13), while the nonrotating case will be governed by equations (6) and (12) with  $f = 0$  in equation (12).

We now cast the equations in nondimensional form by scaling the variables as follows

$$t \rightarrow \frac{d^2}{\kappa} t, \quad (x, y, z) \rightarrow (xd, yd, zd), \quad T \rightarrow T_0 T, \quad w \rightarrow \frac{T_0 \kappa}{\Gamma d^2} w, \quad \text{and}$$

$$\zeta \rightarrow \frac{T_0 \kappa}{\Gamma d^3} \zeta.$$

In dimensionless form the equations are

$$\left( \frac{\partial}{\partial t} - \nabla^2 \right) T = w, \quad (14)$$

$$\left(\frac{1}{\text{Pr}} \frac{\partial}{\partial t} - \nabla^2\right) \nabla^2 w = \text{Ra}(r - z - 1/2) \nabla_H^2 T + \text{Ro} \frac{\partial \zeta}{\partial z}, \quad (15)$$

$$\left(\frac{1}{\text{Pr}} \frac{\partial}{\partial t} - \nabla^2\right) \zeta = -\text{Ro} \frac{\partial w}{\partial z}, \quad (16)$$

where  $\text{Ra} = \alpha g \Gamma^2 d^5 / \nu \kappa$  is the Rayleigh number,  $\text{Pr} = \nu / \kappa$  is the Prandtl number,  $\text{Ro} = fd^2 / \nu$  is a dimensionless rotational parameter, and  $r = (T_1 - T_0) / \Gamma d$  is a positive dimensionless temperature difference parameter.

We next assume normal modes solutions having the form

$$\begin{aligned} w &= \hat{W}(z) e^{ikx + iy + \sigma t}, \\ T &= \hat{T}(z) e^{ikx + iy + \sigma t}, \\ \zeta &= \hat{\zeta}(z) e^{ikx + iy + \sigma t}. \end{aligned} \quad (17)$$

Hence, by using  $\partial / \partial t \rightarrow \sigma$ ,  $\nabla_H^2 \rightarrow -K^2$  and  $\nabla^2 \rightarrow D^2 - K^2$  the amplitudes  $\hat{W}(z)$ ,  $\hat{T}(z)$  and  $\hat{\zeta}(z)$  will satisfy (suppressing the hats)

$$[\sigma - (D^2 - K^2)] T = W, \quad (18)$$

$$\left[\frac{\sigma}{\text{Pr}} - (D^2 - K^2)\right] (D^2 - K^2) W = -\text{Ra} K^2 (r - z - 1/2) T + \text{Ro} D \zeta, \quad (19)$$

$$\left[\frac{\sigma}{\text{Pr}} - (D^2 - K^2)\right] \zeta = -\text{Ro} D W, \quad (20)$$

where  $K^2 = k^2 + l^2$  and  $D$  denotes the differential operator  $d/dz$ .

The amplitude of disturbances having a positive real part for  $\sigma$  will be amplified in time thus indicating instability whereas a negative real part corresponds to stability. A relationship between  $\sigma$  and the parameters  $r$ ,  $\text{Ro}$ ,  $\text{Ra}$ , and  $\text{Pr}$ , for a certain disturbance characterised by the value of  $K$ , can be obtained by regarding equations (18)-(20) as an eigenvalue problem and determining the value of  $\sigma$  for which a nontrivial solution exists. For analytical and numerical purposes the equations will be consolidated into a single equation in subsequent sections. We next discuss the principle of exchange of stabilities for a specified case where it is proved to hold.

### 3.1 Principle of exchange of stabilities

Here it will be shown that in the nonrotating case with free surfaces, if  $\mathcal{R}(\sigma) = 0$  then  $\mathcal{I}(\sigma) = 0$ . Starting with the set of equations for  $W$  and  $T$ , given by equations (18) and (19) with  $\text{Ro} = 0$ , the first step is to combine them to

obtain a single equation for  $T$ . This yields the following sixth order differential equation:

$$D^6 T - \left[ 3K^2 + \left( 1 + \frac{1}{\text{Pr}} \right) \sigma \right] D^4 T + K^2 \left[ 3K^2 + 2 \left( 1 + \frac{1}{\text{Pr}} \right) \sigma \right] D^2 T + \frac{\sigma^2}{\text{Pr}} D^2 T - K^2 \left[ K^4 + \text{Ra} \left( z + \frac{1}{2} - r \right) + \left( 1 + \frac{1}{\text{Pr}} \right) K^2 \sigma + \frac{\sigma^2}{\text{Pr}} \right] T = 0. \quad (21)$$

From the boundary conditions (7) and (8) and the continuity equation (2) we obtain the conditions

$$T = D^2 T = 0 \text{ and } D^3 T = (\sigma + K^2)DT \text{ at } z = \pm 1/2, \quad (22)$$

for the case of rigid surfaces and

$$T = D^2 T = D^4 T = 0 \text{ at } z = \pm 1/2, \quad (23)$$

for the case of free surfaces.

In the above, the only complex quantities are  $T(z)$  and  $\sigma$ . If  $\sigma = \gamma + i\beta$ , we will show that if  $\gamma = 0$  then  $\beta = 0$ ; that is, the marginal state separating stability from instability is given by  $\sigma = 0$ . Taking the complex conjugate, denoted by an asterisk, of equation (21) we obtain

$$D^6 T^* - \left[ 3K^2 + \left( 1 + \frac{1}{\text{Pr}} \right) \sigma^* \right] D^4 T^* + K^2 \left[ 3K^2 + 2 \left( 1 + \frac{1}{\text{Pr}} \right) \sigma^* \right] D^2 T^* + \frac{\sigma^{*2}}{\text{Pr}} D^2 T^* - K^2 \left[ K^4 + \text{Ra} \left( z + \frac{1}{2} - r \right) + \left( 1 + \frac{1}{\text{Pr}} \right) K^2 \sigma^* + \frac{\sigma^{*2}}{\text{Pr}} \right] T^* = 0. \quad (24)$$

Next we multiply equation (21) by  $T^*$  and subtract equation (24) multiplied by  $T$ . This produces the following equation:

$$\begin{aligned}
 & (T^*D^6T - TD^6T^*) - \left[ 3K^2 + \left( 1 + \frac{1}{\text{Pr}} \right) \gamma \right] (T^*D^4T - TD^4T^*) \\
 & - i \left( 1 + \frac{1}{\text{Pr}} \right) \beta (T^*D^4T + TD^4T^*) \\
 & + K^2 \left[ 3K^2 + 2 \left( 1 + \frac{1}{\text{Pr}} \right) \gamma \right] (T^*D^2T - TD^2T^*) \\
 & + \frac{\gamma^2 - \beta^2}{\text{Pr}} (T^*D^2T - TD^2T^*) + i \frac{2\gamma\beta}{\text{Pr}} (T^*D^2T + TD^2T^*) \\
 & + i2K^2 \left( 1 + \frac{1}{\text{Pr}} \right) \beta (T^*D^2T + TD^2T^*) \\
 & - i2K^2 \left[ \left( 1 + \frac{1}{\text{Pr}} \right) K^2 + \frac{2\gamma}{\text{Pr}} \right] \beta TT^* = 0.
 \end{aligned} \tag{25}$$

Making use of some straight-forward algebraic manipulations outlined in the Appendix we obtain the result

$$\begin{aligned}
 & -i\beta \left\{ 2 \left( 1 + \frac{1}{\text{Pr}} \right) \int_{-1/2}^{1/2} |D^2T|^2 dz + 4K^2 \left( 1 + \frac{1}{\text{Pr}} \right) \int_{-1/2}^{1/2} |DT|^2 dz \right. \\
 & \left. + \frac{4\gamma}{\text{Pr}} \int_{-1/2}^{1/2} |DT|^2 dz + 2K^2 \left[ K^2 \left( 1 + \frac{1}{\text{Pr}} \right) + \frac{2\gamma}{\text{Pr}} \right] \int_{-1/2}^{1/2} |T|^2 dz \right\} = 0,
 \end{aligned} \tag{26}$$

for the free surfaces case. Setting  $\gamma = 0$  and noting that everything in the curly brackets is positive, the only way the above equation can be satisfied is if  $\beta = 0$ .

For the rigid surfaces case we get the term

$$(DTD^4T^* - DT^*D^4T) \Big|_{-1/2}^{1/2},$$

appearing on the left-hand-side of equation (26). It is not at all clear whether this term vanishes. As pointed out by Veronis (1963), the principle of exchange of stabilities has not been analytically established for the case of rigid surfaces.

### 3.2 Limiting cases

The study of the stability problem for arbitrary values of the parameter  $r$  requires numerical methods. However, for the limiting cases  $r \rightarrow \infty$  and  $r \rightarrow 0$ ,



and in the absence of rotation an analytic approach can be taken by making use of the principle of exchange of stabilities. Setting  $Ro = 0$  and  $\sigma = 0$ , and combining equations (18) and (19) we obtain for the marginal state the equation

$$(D^2 - K^2)^3 T = -RaK^2(r - \xi)T, \quad (27)$$

where  $\xi = z + 1/2$  and  $D$  now represents the operator  $d/d\xi$ .

We first consider the case  $r \rightarrow \infty$ . This limit corresponds to the density extremum being attained closer and closer to the top of the fluid layer, with the density increasing from the bottom to the top. Therefore, for large values of  $r$  the entire layer is essentially top heavy. Since  $\xi \in [0, 1]$  and we are dealing with the case  $r \rightarrow \infty$ , it follows that  $r \gg \xi$ , and as a result equation (27) can be approximated by

$$(D^2 - K^2)^3 T = -Ra^*K^2T,$$

where  $Ra^* = rRa$ . This equation coincides with the one encountered in the classical problem with  $Ra^*$  as the classical Rayleigh number. Hence the asymptotic formula:

$$Ra \sim \frac{Ra^*}{r} \quad \text{as } r \rightarrow \infty, \quad (28)$$

is easily deduced.

In the limit  $r \rightarrow 0$ , the density extremum is attained closer and closer to the bottom of the layer. Consequently, we have a top-heavy stratification only in a thin layer near the bottom. This then suggests approximating equation (27) by setting  $\xi = 0$ , as  $\xi = 0$  corresponds to the bottom of the layer. Also, it is appropriate to rescale the problem as follows. We first point out that  $\bar{T} = T_0$  when  $\xi = r$  and so the top-heavy stratification is contained in a region of thickness  $r$ . Thus, we rescale the vertical coordinate according to  $\xi = r\chi$ . Equation (27) then simplifies to

$$(\tilde{D}^2 - \tilde{K}^2)^3 T = -Ra^*\tilde{K}^2T,$$

where  $Ra^* = r^5Ra$ ,  $\tilde{D} \equiv d/d\chi$ , and  $\tilde{K} = rK$  which, once again, is the equation governing the disturbances in the classical problem. It then follows that the asymptotic form for small  $r$  is

$$Ra \sim \frac{Ra^*}{r^5} \quad \text{as } r \rightarrow 0. \quad (29)$$

In the next section we will numerically confirm the validity of the principle of exchange of stabilities and compare the results with the asymptotic forms for both large  $r$  and small  $r$ .

#### 4. Numerical methods and results

Our goal is to establish the dependence of the complex growth rate  $\sigma$  with the other parameters of the problem. By analyzing the variation of  $\sigma$  we will be able to draw conclusions regarding the conditions under which instability occurs. We will also be able to investigate the validity of the principle of exchange of stabilities and verify whether neutral stability coincides with marginal stability.

To obtain numerical results we consider the problem governing the amplitude of the temperature disturbance which in the nonrotating case is given by equation (21) together with conditions (22) for the rigid surfaces case and conditions (23) for the free surfaces case. For the rotating case with free surfaces the governing problem is dictated by

$$\begin{aligned}
 & D^8 T - \left[ 4K^2 + \left( 1 + \frac{2}{\text{Pr}} \right) \sigma \right] D^6 T \\
 & + \left[ 6K^4 + 3 \left( 1 + \frac{2}{\text{Pr}} \right) K^2 \sigma + \left( 2 + \frac{1}{\text{Pr}} \right) \frac{\sigma^2}{\text{Pr}} + \text{Ro}^2 \right] D^4 T \\
 & - \left\{ 4K^6 + 3 \left( 1 + \frac{2}{\text{Pr}} \right) K^4 \sigma + 2 \left( 2 + \frac{1}{\text{Pr}} \right) \frac{\sigma^2 K^2}{\text{Pr}} \right. \\
 & \left. + \left[ \text{Ro}^2 + \text{Ra} \left( z + \frac{1}{2} - r \right) \right] K^2 + \frac{\sigma^3}{\text{Pr}^2} + \text{Ro}^2 \sigma \right\} D^2 T \\
 & - 2\text{Ra}K^2 D T + K^2 \left[ K^6 + \left( 1 + \frac{2}{\text{Pr}} \right) K^4 \sigma + \left( 2 + \frac{1}{\text{Pr}} \right) \frac{\sigma^2 K^2}{\text{Pr}} \right. \\
 & \left. + \frac{\sigma^3}{\text{Pr}^2} + \text{Ra} \left( z + \frac{1}{2} - r \right) \left( \frac{\sigma}{\text{Pr}} + K^2 \right) \right] T = 0.
 \end{aligned}$$

along with the conditions

$$D^6 T = D^4 T = D^2 T = T = 0 \quad \text{at} \quad z = \pm 1/2.$$

We will apply two methods to obtain the eigenvalues to the above-mentioned problems. One consists of expanding  $T(z)$  in a truncated eigenfunction series while the other approach is to use a truncated power series.

The eigenfunction expansion of the form

$$T(z) = \sum_{j=1}^n B_j \sin [j\pi(z + 1/2)]$$

is appropriate for the free surfaces case since the eigenfunctions  $\{\sin [j\pi(z + 1/2)]\}_{j=1}^n$  satisfy the boundary conditions. Subsequent to substituting this expansion for  $T(z)$  into the governing differential equation we multiply the equation by  $\sin [m\pi(z + 1/2)]$ , for  $m = 1, 2, \dots, n$  and integrate with respect to  $z$  from  $-1/2$  to  $1/2$ . This yields a homogeneous system of  $n$  algebraic equations for the coefficients  $B_j$ . For example, in the nonrotating case the system becomes

$$\sum_{j=1}^n \{[(j^2\pi^2 + K^2)^3 + (\sigma/\text{Pr} + \sigma)(j^2\pi^2 + K^2)^2 + \sigma^2/\text{Pr}(j^2\pi^2 + K^2) - r\text{Ra}K^2 + 1/2\text{Ra}K^2]\delta_{mj} + 2\text{Ra}K^2I_{mj}(1 - \delta_{mj})\}B_j = 0, \quad m = 1, 2, \dots, n,$$

where  $\delta_{mj}$  is the Kronecker delta and

$$I_{mj} = \begin{cases} \frac{-4mj}{\pi^2(m^2 - j^2)^2} & \text{if } m + j \text{ is odd} \\ 0 & \text{if } m + j \text{ is even.} \end{cases}$$

Since the eigenfunctions used in the above expansion do not satisfy the boundary conditions which apply to the rigid surfaces case, we consider a truncated power series expansion of the form

$$T(z) = \sum_{j=0}^{n-1} \frac{a_j}{j!} z^j.$$

Substituting this expansion into the governing differential equation and equating the coefficients of powers of  $z$  to zero, we obtain the following recurrence relation for the coefficients  $a_j$ :

$$j\text{Ra}K^2a_{j-1} - K^2[\text{Ra}(r - 1/2) - (\sigma/\text{Pr} + K^2)(\sigma + K^2)]a_j - [K^2(\sigma + K^2) + (\sigma/\text{Pr} + K^2)(\sigma + 2K^2)]a_{j+2} + (\sigma/\text{Pr} + \sigma + 3K^2)a_{j+4} + a_{j+6} = 0, \quad j = 0, \dots, n - 7.$$

Using this relation and the boundary conditions we again obtain a homogeneous systems of  $n$  algebraic equations for the coefficients. We point out that the truncated power series method can also be used for the free surfaces case, thus allowing us to compare the results obtained using the two methods.

---

For both the expansion methods, equating the determinant of the coefficient matrix of the algebraic system to zero enables us to solve for  $\sigma$ . The determinant was numerically computed using the IMSL routine DLFDCB. Then the IMSL routine DZANLY was applied to obtain the roots of the dispersion equation. Particularly, we are only interested in the root having the largest real part. This routine uses Müller's method which can be regarded as a generalization of the Secant method. While the Secant method uses two initial approximations to linearly estimate the roots of a polynomial, Müller's method uses three approximations to quadratically estimate the roots. The details of this method are presented in Müller's original paper (Müller, 1956) as well as in texts on numerical analysis such as Burden and Faires (1985). The advantage offered by Müller's method is that the technique, in general, will converge for any initial approximation. However, Müller's method is not quite as efficient as Newton's method. Its order of convergence near a root is  $\sim 1.84$  compared to Newton's method which is 2; but, it is better than the Secant method whose order is  $\sim 1.62$ . The stopping criterion of the routine DZANLY is the size of the relative error between successive approximations to the root. This relative error was set to  $10^{-15}$  which is the accuracy of the computer's double-precision.

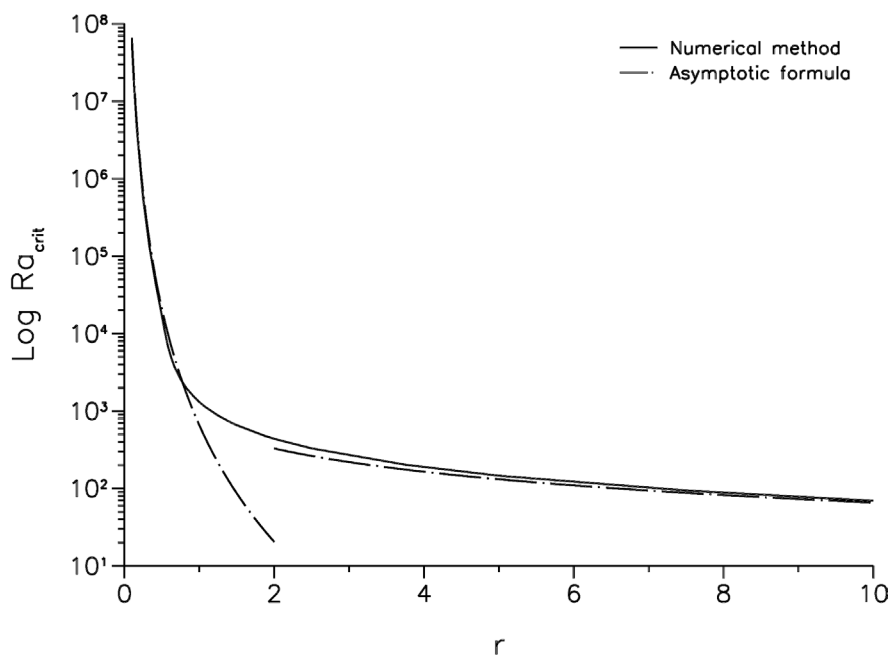
In order to test our numerical method we have compared the numerical results with exact analytical results for the classical Bénard problem where the fluid layer is not rotating and the density is assumed to vary linearly with the temperature. For example, for the free surfaces case the exact analytical equation for the curve of neutral stability is (Drazin and Reid, 1981)  $Ra = (\pi^2 + K^2)^3 / K^2$ . Excellent agreement between this curve and the numerical results was observed. In particular, the numerically determined critical Rayleigh number and corresponding value of  $K$  are  $Ra_{\text{crit}} = 658$  and  $K_{\text{crit}} = 2.21$ , while the exact values are  $Ra_{\text{crit}} = 27\pi^4/4 \approx 657.5$  and  $K_{\text{crit}} = \pi/\sqrt{2} \approx 2.22$ .

Comparisons have also been made between the numerical results and the asymptotic forms given by equations (28) and (29). Presented in Figures 2 and 3 are graphs of the critical Rayleigh number as a function of  $r$  for the nonrotating free surfaces case and the nonrotating rigid surfaces case, respectively. It is clear from these diagrams that the numerically determined  $Ra_{\text{crit}}$  approaches the analytically determined asymptotic behavior for both small  $r$  and large  $r$ .

We next compare the results obtained from the two expansion methods for  $T(z)$ . Figure 4 shows the growth rate  $\mathcal{R}(\sigma)$  as a function of  $K$  using various number of terms retained in the series. The figure demonstrates the excellent agreement between the two expansion methods and also that the series converge fairly rapidly. We also point out that numerical experiments have verified that the growth rate is a strictly monotone function of  $K$  in the neighbourhood of a root. This is a strong evidence that the neutrally stable state is, in fact, marginally stable.

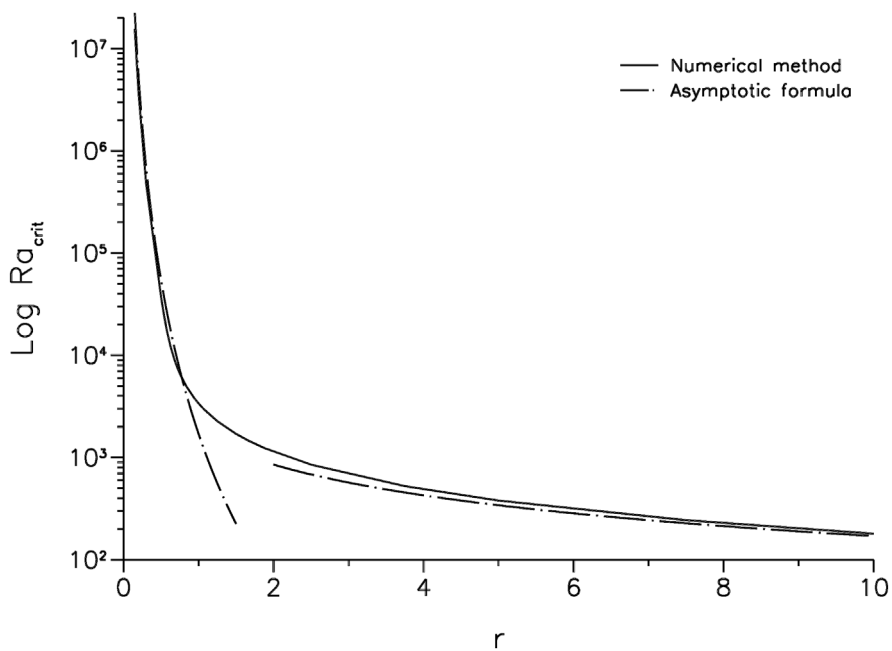
**Figure 2.**  
Variation of the critical Rayleigh number with  $r$  for the nonrotating free surfaces case with  $Pr = 11.6$

---



**Figure 3.**  
Variation of the critical Rayleigh number with  $r$  for the nonrotating case with rigid surfaces with  $Pr = 11.6$

---



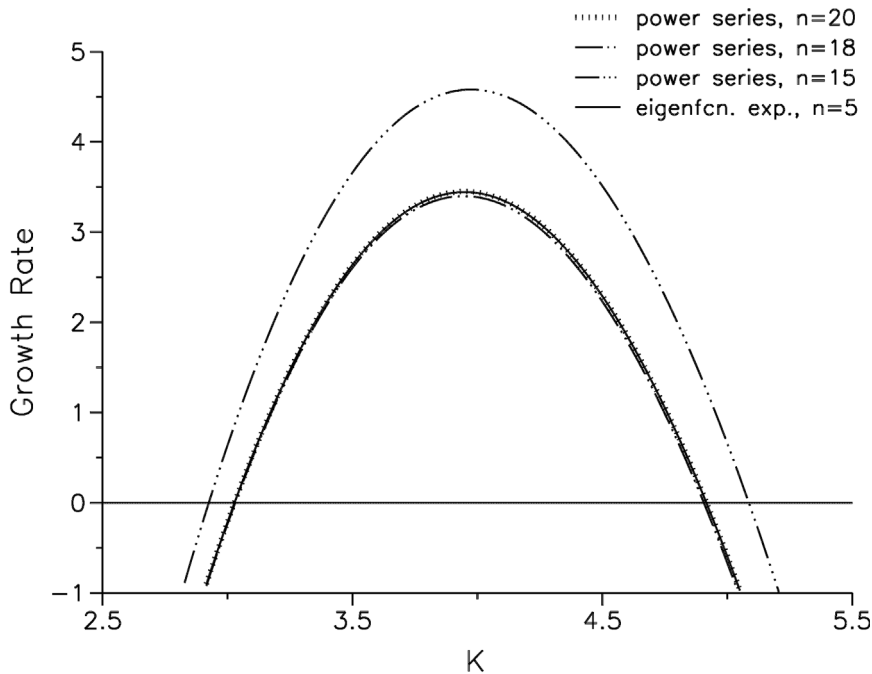


**Figure 4.**  
Variation of the growth  
rate with  $K$  for the free  
surfaces case with no  
rotation,  $r = 0.42$ ,  
 $Ra = 46,000$ , and  
 $Pr = 11.6$

The validity of the principle of exchange of stabilities can be verified by determining if  $\mathcal{I}(\sigma) = 0$  when  $\mathcal{R}(\sigma) = 0$ . Our numerical investigation indicates that the principle of exchange of stabilities is valid in the absence of rotation for both the case of free surfaces and the case of rigid surfaces. Also, as in the case of the classical Bénard problem, numerical experiments demonstrated that the marginal stability curves showed very little sensitivity to the Prandtl number. This further supports the validity of the principle of exchange of stabilities since when  $\sigma = 0$  the Pr dependence vanishes.

For the rotating case with free surfaces and a linear dependence between density and temperature, it has been shown (Chandrasekhar, 1981) that the principle of exchange of stabilities is valid only if  $Pr \geq 1$ . For the case  $Pr < 1$  an important question is whether, under the critical conditions for the onset of instability, the instability manifests itself as stationary convection or as oscillations having a growing amplitude (referred to as “overstability”). It turns out that there is a critical Prandtl number  $Pr^*$  ( $Pr^* = 0.6766$  for the case of free surfaces) such that for  $Pr \geq Pr^*$  the onset of instability is manifested as stationary convection. In other words, for this range of Pr values, at the onset of instability  $\mathcal{I}(\sigma) = 0$ , and furthermore, as a result the critical conditions are independent of Pr. For  $Pr < Pr^*$ , on the other hand, there is a critical relationship between Pr and the rotational parameter Ro such that the onset of instability is manifested as overstability if Pr is sufficiently small or if Ro

is sufficiently large. We have found that as  $r$  was increased, and thus our model approaches the classical one, the results approach those of Chandrasekhar.

Now, by decreasing the value of  $r$  we can gauge the effect of the density extremum on the type of instability at the onset of instability. Our results indicate that the density extremum suppresses the onset of instability as overstability. More specifically, there is a critical value of  $r$  (say  $r^*$ ) such that if  $r < r^*$  the onset of instability occurs as stationary convection rather than overstability. This fact is illustrated by the marginal stability curves presented in Figures 5 and 6. Our numerical experiments indicate that  $r^*$  is a decreasing function of  $Ro$  and an increasing function of  $Pr$ .

In order to investigate the effect of the density extremum on the onset of thermal instability we have determined the variation of the critical Rayleigh number as a function of the parameter  $r$ . Recall that as  $r$  decreases, the position where the density extremum is attained by the basic state moves downward and therefore reduces the thickness of the top-heavy region formed at the bottom of the fluid layer. As a result, we expect that decreasing  $r$  has a stabilizing effect. Indeed, the results presented in Figures 2, 3, and 7 indicate that  $Ra_{crit}$  is a decreasing function of  $r$  in all cases. The variation of the critical  $K$  value with  $r$  is listed in Table I.

The results in Figures 2 and 3 also indicate that a fluid layer confined between free surfaces is more unstable than one confined between rigid surfaces as is the case for the classical Bénard problem. Furthermore, as it can

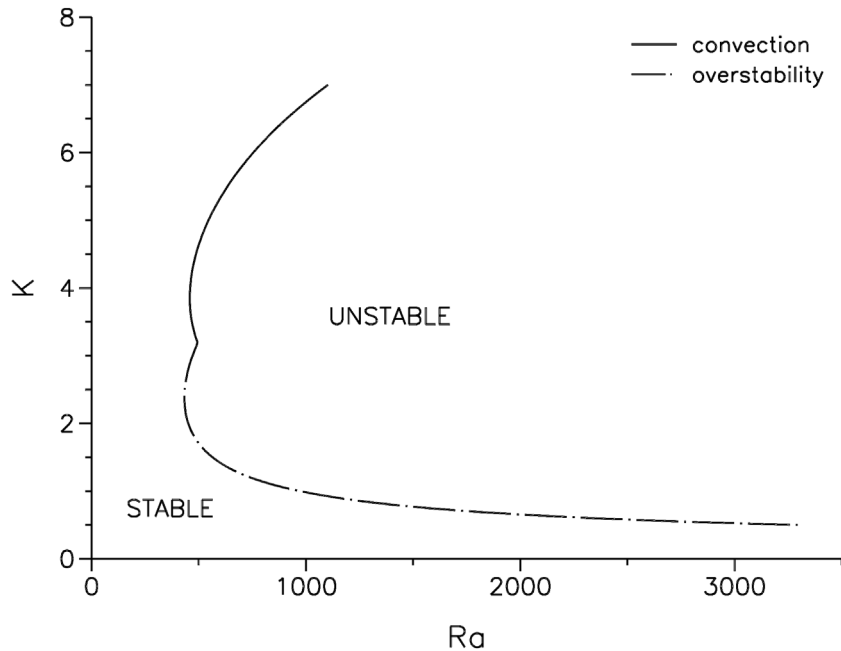


**Figure 5.**  
Marginal stability curve  
for the free surfaces case  
with  $r = 5$ ,  $Pr = 0.2$ , and  
 $Ro = 35$

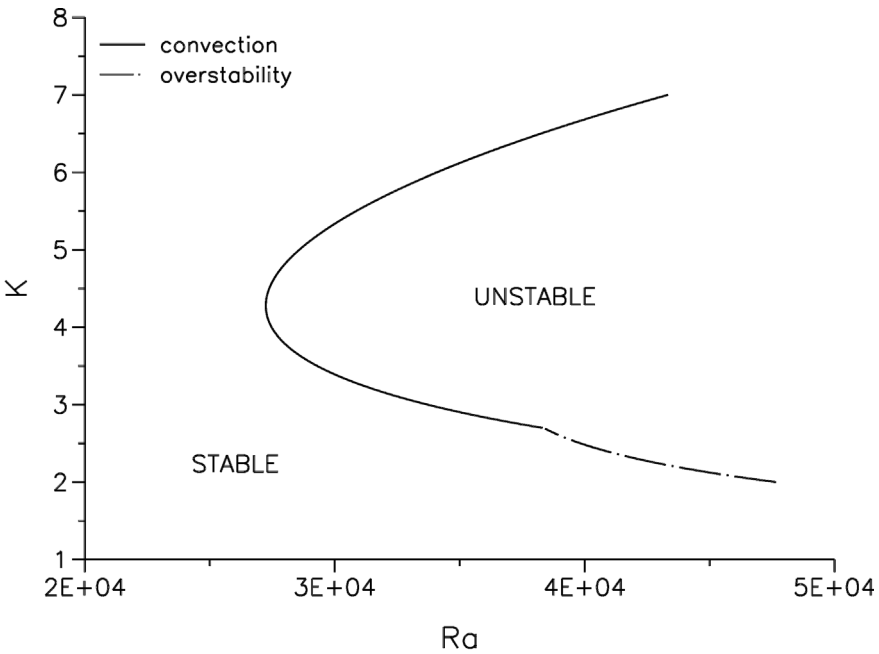


**Figure 6.** Marginal stability curve for the free surfaces case with  $r = 1$ ,  $Pr = 0.2$ , and  $Ro = 35$

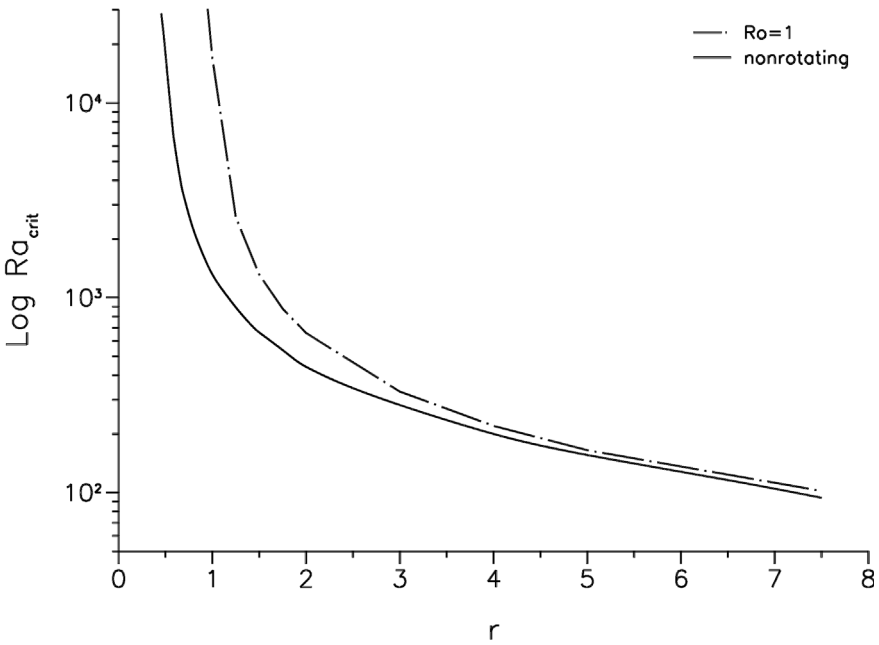


**Figure 7.** Variation of the critical Rayleigh number with  $r$  for the free surfaces case with  $Pr = 11.6$



**Table I.**  
Critical  $K$  values for  
the nonrotating case  
with  $Pr = 11.6$

$r$	Free surfaces		Rigid surfaces	
	$Ra_{crit}$	$K_{crit}$	$Ra_{crit}$	$K_{crit}$
0.42	44,333	3.88	94,163	4.91
0.45	28,732	3.53	61,137	4.5
0.5	16,995	3.02	37,326	4.11
0.54	11,123	2.63	25,726	3.65
0.58	7,206	2.63	17,564	3.39
0.62	4,889	2.3	12,290	3.25
0.68	3,488	2.26	8,923	3.21
0.75	2,580	2.24	6,634	3.15
1.0	1,309	2.24	3,390	3.12
7.5	94	2.21	244	3.11

be seen from Figure 8 the region of instability in the  $Ra - K$  plane is larger for the free surfaces case. In particular, for all supercritical  $Ra$  values a larger range of modes are unstable in the free surfaces case when compared with the rigid surfaces case.

The variation of the critical disturbances with  $z$  is shown in Figure 9. This graph shows the  $z$  dependence of the amplitude of the temperature disturbance  $T(z)$ , scaled by its maximum value. As previously explained, small values of  $r$  correspond to situations in which the region of top-heavy stratification near

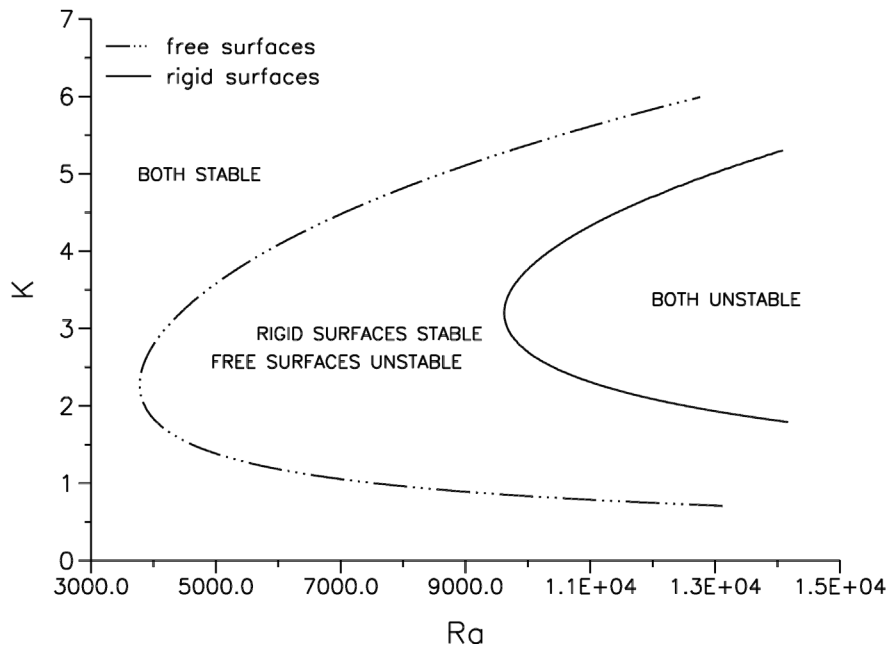


**Figure 8.**  
Marginal stability curves  
for the nonrotating case  
with  $r = 0.67$  and  
 $Pr = 11.6$

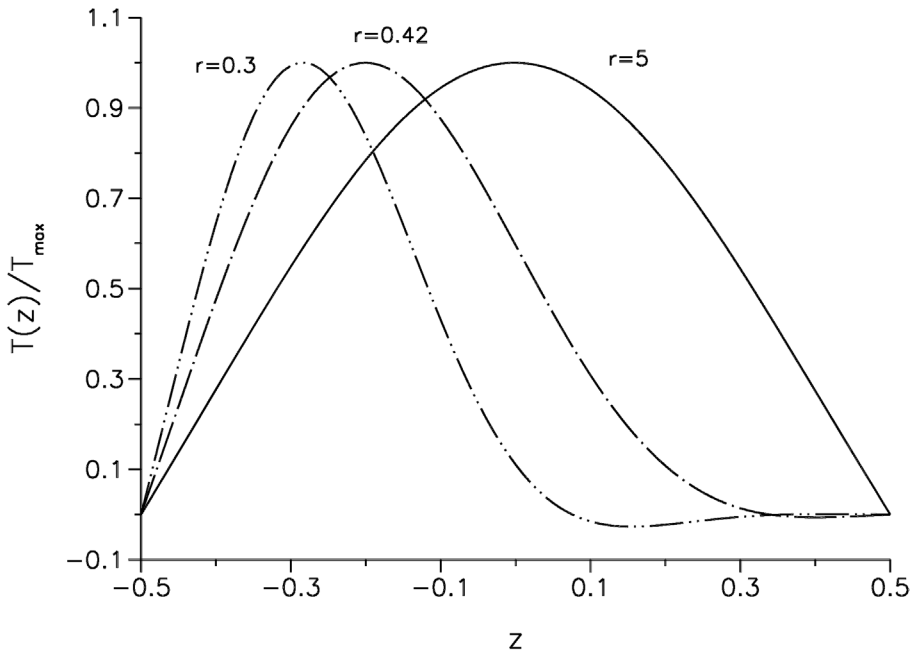


**Figure 9.**  
Scaled amplitude of  
the critical temperature  
disturbance for the  
nonrotating rigid  
surfaces case with  
 $Pr = 11.6$

the bottom surface is relatively thin. Accordingly, as  $r$  decreases the disturbance distribution becomes skewed towards the bottom of the fluid layer.

Lastly, to assess the effect of rotation on the thermal instability we compare the results obtained for the nonrotating case with those obtained having various values of the parameter  $Ro$ . The results presented in Figure 7 indicate that a rotating layer is more stable than a nonrotating one. This is confirmed by the marginal stability curves presented in Figure 10 which indicate that the critical Rayleigh number increases with  $Ro$  as does the region of stability in the  $Ra - K$  plane.

## 5. Summary

Two stability problems related to the classical Bénard convection problem have been presented. Both problems involve a fluid possessing a density extremum with a quadratic equation of state. In one problem the fluid layer is stationary while in the other the entire configuration is allowed to rotate about the  $z$ -axis. The boundary surfaces were assumed to be either free surfaces or rigid surfaces.

As revealed by the numerical results, both rotation and the presence of a density extremum have a stabilizing effect on the thermal convection problem. This can be explained as follows. Rotation acts so as to suppress vertical motion, and hence thermal convection, by restricting the motion to the horizontal plane. The partial stable stratification in the layer, which occurs

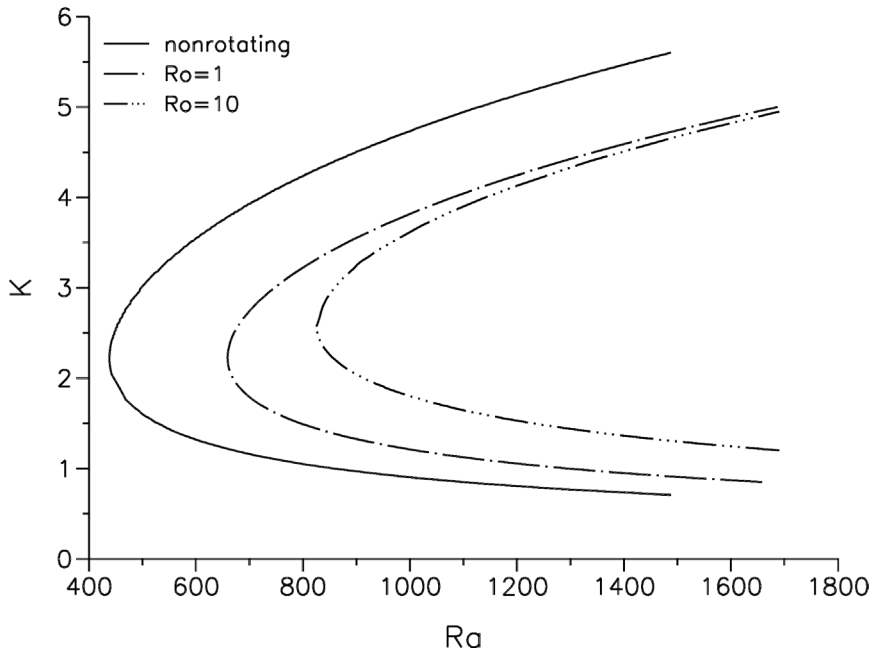


**Figure 10.**  
Marginal stability curves  
for the free surfaces case  
with  $r = 2$  and  $Pr = 11.6$

when the density extremum lies between the top and bottom of the fluid layer, further acts to reduce vertical velocities. This combined effect attempts to impose a two-dimensional nature on the flow, confining the motion to the horizontal plane. An additional effect of the density extremum is to allow the onset of stationary convection instead of oscillatory instability which is associated with small Prandtl numbers and fast rotation.

### References

- Bénard, H. (1900), "Les tourbillons cellulaires dans une mappe liquide", *Rev. Gen. Sci. Pures Appl.*, Vol. 11, pp. 1261-71.
- Burden, R.L. and Faires, J.D. (1985), *Numerical Analysis*, 3rd ed., Prindle, Weber and Schmidt Pub., Boston.
- Chandrasekhar, S. (1981), *Hydrodynamic and Hydromagnetic Stability*, Dover Pub., New York.
- Drazin, P.G. and Reid, W.H. (1981), *Hydrodynamic Stability*, Cambridge University Press, Cambridge.
- Eklund, H. (1963), "Freshwater: temperature of maximum density calculated from compressibility", *Science*, Vol. 142, pp. 1457-8.
- Hwang, L-T., Lu, W-F. and Mollendorf, J.C. (1984), "The effects of the density extremum and boundary conditions on the stability of a horizontally confined water layer", *Int. J. Heat Mass Transfer*, Vol. 27, pp. 497-510.
- Mollendorf, J.C. and Jahn, K.H. (1983), "Onset of convection in a horizontal layer of cold water", *ASME J. Heat Transfer*, Vol. 105, pp. 460-4.

- Müller, D.E. (1956), "A method for solving algebraic equations using an automatic computer", *Mathematical Tables and Aids to Computation*, Vol. 10, pp. 208-15.
- Rayleigh, L. (1916), "On convection currents in a horizontal layer of fluid when the higher temperature is on the under side", *Phil. Mag.*, Vol. 32, pp. 529-46.
- Veronis, G. (1963), "Penetrative convection", *Astrophysical J.*, Vol. 137, pp. 641-63.

### Appendix

For simplifying equation (25) we made use of the following identities:

$$T^*D^6T - TD^6T^* = D[T^*D^5T - TD^5T^*] + D[DTD^4T^* - DT^*D^4T] \\ + D[D^2T^*D^3T - D^2TD^3T^*],$$

$$T^*D^4T - TD^4T^* = D[T^*D^3T - TD^3T^*] + D[DTD^2T^* - DT^*D^2T],$$

$$T^*D^2T - TD^2T^* = D[T^*DT - TDT^*],$$

$$T^*D^2T + TD^2T^* = D[T^*DT + TDT^*] - 2DT^*DT,$$

$$T^*D^4T + TD^4T^* = D[T^*D^3T + TD^3T^*] - D[DT^*D^2T + DTD^2T^*] + 2D^2T^*D^2T.$$

Equation (25) was integrated term-by-term from  $z = -1/2$  to  $z = 1/2$ . Owing to the boundary conditions (22) and (23), each of the integrated terms become:

$$\int_{-1/2}^{1/2} (T^*D^6T - TD^6T^*) dz = \begin{cases} 0 & \text{for free surfaces case} \\ (DTD^4T^* - DT^*D^4T)|_{-1/2}^{1/2} & \text{for rigid surfaces case} \end{cases}$$

$$\int_{-1/2}^{1/2} (T^*D^4T - TD^4T^*) dz = 0 \text{ for both cases,}$$

$$\int_{-1/2}^{1/2} (T^*D^4T + TD^4T^*) dz = 2 \int_{-1/2}^{1/2} |D^2T|^2 dz \text{ for both cases,}$$

$$\int_{-1/2}^{1/2} (T^*D^2T - TD^2T^*) dz = 0 \text{ for both cases,}$$

$$\int_{-1/2}^{1/2} (T^*D^2T + TD^2T^*) dz = -2 \int_{-1/2}^{1/2} |DT|^2 dz \text{ for both cases.}$$